
A LATENT VARIABLE APPROACH TO ACCOUNT FOR CORRELATED INPUTS IN GLOBAL SENSITIVITY ANALYSIS WITH CASES FROM PHARMACOLOGICAL SYSTEMS MODELLING

A PREPRINT

Nicola Melillo

Centre for Applied Pharmacokinetic Research
School of Health Sciences
The University of Manchester
Manchester, UK
nicola.melillo@manchester.ac.uk

Adam S. Darwich

Division of Health Informatics and Logistics
Department of Biomedical Engineering and Health Systems
KTH Royal Institute of Technology
Stockholm, Sweden
darwich@kth.se

December 7, 2020

ABSTRACT

In pharmaceutical research and development decision-making related to drug candidate selection, efficacy and safety is commonly supported through modelling and simulation (M&S). Among others, physiologically-based pharmacokinetic models are used to describe drug absorption, distribution and metabolism in human. Global sensitivity analysis (GSA) is gaining interest in the pharmacological M&S community as an important element for quality assessment of model-based inference. Physiological models often present inter-correlated parameters. The inclusion of correlated factors in GSA and the sensitivity indices interpretation has proven an issue for these models. Here we devise and evaluate a latent variable approach for dealing with correlated factors in GSA. This approach describes the correlation between two model inputs through the causal relationship of three independent factors: the latent variable and the unique variances of the two correlated parameters. Then, GSA is performed with the classical variance-based method. We applied the latent variable approach to a set of algebraic models and a case from physiologically-based pharmacokinetics. Then, we compared our approach to Sobol's GSA assuming no correlations, Sobol's GSA with groups and the Kucherenko approach. The relative ease of implementation and interpretation makes this a simple approach for carrying out GSA for models with correlated input factors.

Keywords latent variable · correlated factors · global sensitivity analysis · physiologically based pharmacokinetic models · systems modelling · model-informed drug discovery and development

1 Introduction

The use of sensitivity analysis (SA), including global SA (GSA), has gained interest from pharmaceutical industry, regulators and academia in recent years [1, 2, 3, 4, 5, 6, 7, 8, 9, 10]. In pharmaceutical research and development (R&D) decision-making for drug candidate selection, efficacy and safety is often supported by modelling and simulation (M&S). This is referred to as **model-informed drug discovery and development (MID3)** [11]. SA is an indispensable instrument for the quality assessment of model-based inference [12]. However, it is the authors' opinion, that the treatment and interpretation of correlated input parameters in GSA can be a barrier to wider use.

1.1 Modelling for decision-making in pharmaceutical R&D

Broadly, modelling activities in pharmaceutical R&D are centred around the study of disease, pharmacokinetics (PK; *in vivo* drug absorption, distribution, metabolism and elimination, or ADME), structure-activity relationships, pharmacodynamics (PD; temporal pharmacological effects) and more [11]. In this work, we focus on PK models.

PK models vary in complexity, ranging from simple empirical models, to complex models based on physiological considerations [13, 14]. Empirical PK models use functions, such as sum of exponential terms, to describe the drug concentration-time profiles. In these models the parameters are generally estimated from the data and have no clear physiological meaning. Here we focus on the class of physiologically-based models, such as systems models of biology, disease and pharmacology, that are applied throughout drug development. As these models are based on physiological mechanisms, they can be used to extrapolate PK/PD effects from *in vitro* to *in vivo*, between species, populations and scenarios [15].

Physiologically-based pharmacokinetic (PBPK) M&S provides a framework for mechanistic predictions of PK. PBPK models consist of systems of ordinary differential equations based on mass balance (see also physiologically-based toxicokinetics [16]). PBPK models are compartmental models in which each compartment corresponds to a specific organ or tissue and is connected to other compartments through flow rates representing the blood circulation. This structure reflects a representation of the true anatomical layout. Data on population demographics, tissue composition, organ function, drug metabolising enzymes, transporters and whole blood parameters are integrated with drug and formulation-specific information to predict drug exposure over time [17]. PBPK M&S has been used to replace/supplement clinical trials and inform labelling for numerous drugs, most notably for dosage recommendations following metabolic drug-drug interactions [18, 19], avoiding adverse effects in patients.

Uncertainty and variability are prominent in biological data and an important consideration for decisions on drug safety. For example, during drug development, when the drug is administered for the first time in humans (so called, first-in-human trials), uncertainty affects the probability in risk predictions, therefore informing the dosing strategy. In this context, uncertainty mainly relates to inter- and intra-experimental variability, experimental errors in laboratory and physiological measures, and translation of parameters. Variability mainly relates to interindividual variability in physiology, protein expression, genetics, interoccasion variability and more.

Correlations between input parameters are often implemented in PBPK models to account for physiological constraints, otherwise causing implausible combinations of parameters [20, 21]. For example, organ weights and blood flows are constrained by body weight and cardiac output. With the emergence of novel 'omics techniques, the correlation of proteins is also of increasing interest [22, 23].

1.2 Global sensitivity analysis for PBPK M&S: the issue of correlated input factors

Both the United States Food and Drug Administration (FDA) and European Medicines Agency (EMA) have highlighted the importance of SA and GSA as best practice in PBPK to inform model development and refinement [1, 2]. GSA is key for elucidating the relationship between the uncertainty and variability in model inputs and variation in a given model output. Therefore, by extension, the method is also relevant for drug development and precision dosing in clinical practice [3, 4, 9, 24, 25].

In this work, we focused on the variance-based GSA (also referred to as Sobol's method) [3, 5]. This choice was made as the variance-based GSA is able to handle nonlinear and nonmonotonic relationships between the input factors and the model outputs [26, 27, 28]. Moreover, with this method it is possible to quantify the effect of each factor taken singularly and the extent of its interaction effects. As we have reported in previous work, understanding the extent of the interaction effects can be particularly important for an informed use of PBPK models during drug development [5].

The classical variance-based GSA works under the assumption that model inputs (commonly referred to as model parameters in pharmacometrics) are independent [26, 28, 27]. Under this assumption, the variance decomposition is unique [26] and reflects the structure of the model itself [29]. In this context, the variance-based sensitivity indices

have a clear interpretation [27, 30]. However, most PBPK models violate the independence assumption [4, 20, 31]. In practice this may lead to correlations being ignored in the analysis, or the use of one of several proposed methods for GSA that deal with dependent inputs. Perhaps, the most simple and elegant way of treating dependent inputs in GSA is by grouping the correlated factors and then performing a GSA with the independent groups. The intrinsic limitation of this approach is that it is not possible to distinguish the contribution of the single variables within each group.

In the literature, several methods have been developed to deal with dependent inputs while retaining the information, or sensitivity indices, of each individual factor. These methods typically fall into one of two classes: parametric and non-parametric methods [32, 33]. The parametric methods, also called model-based methods, (e.g., [34, 35, 36]) assume an *a priori* model for the input-output relation. Instead, the non-parametric approaches do not assume any specific shape for this relation and thus, they are referred to as model-free or non model-based methods [33, 32]. These approaches are by and large considered more suitable for computer-based modelling [33]. Generally, the non-parametric methods employ a transformation technique for dealing with correlated factors' distribution [33]. For example, Kucherenko *et al.* [37] used copula transformations to generalise the first order and total Sobol indices for the case of dependent input factors. Mara *et al.* [32] proposed the use of the Rosenblatt transformation, and Tarantola and Mara [38] used both the Rosenblatt and Nataf transformation within the context of variance-based GSA. Moreover, other methods such as the variogram analysis of response surfaces (VARS) and the Shapely effects have been extended for the case of correlated input factors [33, 30].

The copula-based method, developed by Kucherenko and coworkers [37], has recently been proposed for PBPK models and implemented in a commercial PBPK software [31, 39]. However, how to interpret variance-based GSA results in presence of dependent variables is not straightforward and still debated among GSA practitioners. In presence of correlation between the input factors, the correspondence between the variance-based indices and model structure is lost and the variance decomposition can no longer provide a description of the model structure [29, 40, 41]. This was illustrated by Oakley and O'Hagan in 2004 with the use of a simple example [29]. In this context, Pianosi *et al.* reported that '*counterintuitive results may be obtained*' [41]. Iooss and Lemaître reported that '*SA for dependent inputs has also been discussed by several authors [...], but this issue remains misunderstood*' [42]. Moreover, Iooss and Prieur reported that '*The so-called Sobol' indices [...], present a difficult interpretation in the presence of statistical dependence between inputs*' [30].

Several dedicated software platforms exist for PBPK M&S [43], providing accessible tools for non-expert users. As GSA gains use in the community (such as through software implementation) the issue of interpretability becomes increasingly relevant.

Here we propose a latent variable approach for treating correlated input parameters in variance-based GSA. The method expresses the correlation between two parameters as causal relationships between uncorrelated variables. This is done in order to allow the use of classical variance-based GSA and avoids the usage of methods whose interpretation is still a matter of debate. Latent variable models and sub-varieties of them, such as factor analysis, path analysis and structural equation modelling, are widely used in social sciences [44]. In latent variable models, the correlation between more than one observed measure (or model parameter) is described by one, or more, unobserved (latent) variable(s). Parameters are correlated as they share a common cause [45]. Here we focus on the case of two linearly correlated random variables whose correlation is explained by one latent variable. With this approach, instead of two correlated factors, three independent factors (the latent variable and the two independent variances of the correlated parameters) are considered in the GSA.

The approach is then applied to a set of algebraic models and a whole-body PBPK model for the drug midazolam (MDZ). MDZ is a sedative primarily metabolised by Cytochrome P450 (CYP) 3A4 and CYP3A5 [46]. The expression of CYP3A5 is polymorphic and present in around 10-20% [47] of Caucasians where it is correlated with CYP3A4 through a shared mechanism for expression [48]. The latent variable approach was then compared with the classic Sobol's variance-based GSA, Sobol's GSA performed by grouping together the correlated factors, and the Kucherenko approach.

2 Materials and Methods

2.1 Variance-based sensitivity analysis and the Kucherenko approach

Let us consider the generic model in Equation 1:

$$Y = f(\mathbf{X}), \quad (1)$$

where Y is the scalar model output, \mathbf{X} is the vector including the k independent input factors ($X_i, i = 1 \dots k$) and f is the input-output relationship. In variance-based GSA (also known as Sobol's GSA) two sensitivity indices are derived from the decomposition of the variance (V) of Y . These are the so called first order index (or main effect) S_i and the total effect ($S_{T,i}$), in Equation system 2 [26, 28, 49].

$$\begin{aligned} S_i &= \frac{V_{X_i}(E_{\mathbf{X}_{\sim i}}(Y | X_i))}{V(Y)} \\ S_{T,i} &= \frac{E_{\mathbf{X}_{\sim i}}(V_{X_i}(Y | \mathbf{X}_{\sim i}))}{V(Y)} \end{aligned} \quad (2)$$

$\mathbf{X}_{\sim i}$ represents a vector including all the factors except X_i , while E is the expectation operator. S_i is related with the part of $V(Y)$ explained by the variation of X_i taken singularly and $S_{T,i}$ is the sum of S_i with all the interaction effects of X_i with the other inputs [27, 28]. When the parameters are independent, the relationships $S_i \leq S_{T,i}$ and $\sum S_i \leq 1$ are always valid and $S_{T,i} - S_i$ gives information about the extent of interaction effects involving X_i [27, 28].

The GSA method proposed by Kucherenko *et al.* [37] can consider models with dependent input factors. Here, the main and total effects of the variance-based GSA are calculated with a copula-based method. With this approach, S_i includes the effects of the dependence of X_i with other factors [32] and can be higher than $S_{T,i}$. As reported by [32], $S_{T,i}$ includes only the effects of X_i that are not due to its dependence with $\mathbf{X}_{\sim i}$. A given factor whose importance is only due to the correlation with another factor would have $S_{T,i} = 0$, but S_i can be different from 0 [32]. Moreover, $S_{T,i}$ approaches 0 as the correlation $|\rho| \rightarrow 1$ [37]. A possible explanation for this behaviour is that as the correlation approaches 1, the value of X_i is completely informed by $\mathbf{X}_{\sim i}$ and thus $V_{X_i}(Y | \mathbf{X}_{\sim i})$ will tend to 0.

2.2 Latent variable approach for GSA

This approach expresses the inter-correlation between two parameters as causal relationships between uncorrelated variables. Therefore allowing the use of classical variance-based GSA.

Latent variable methods partition the *observed variance* of each correlated parameter (observed variable) into two parts: a *common variance*, caused by the latent variable and a *unique variance*, specific to the parameter itself [45]. In this work, we focus on the case of two linearly correlated random variables whose correlation is explained by one latent variable. The relationship between the observed, common and unique variances for two correlated parameters and one latent variable is reported through a path diagram as shown in Figure 1 [44]. Following the notation of latent-variable methodology, η is the latent variable, and is conventionally represented by a circle in the path diagram. Unidirectional arrows represent the causal relationships between latent and dependent factors $X_i, i = 1, 2$ (depicted by a box) and ε_i represents the unique variance associated with X_i [45]. X_1 and X_2 are considered linearly correlated, with a linear (Pearson) correlation coefficient of ρ_{12} . Here we assume that η, X_i and ε_i are distributed as in Equation system 3 and that η and ε_i are independent.

$$\begin{aligned} \eta &\sim \mathcal{N}(0, 1) \\ X_i &\sim \mathcal{N}(0, 1) \\ \varepsilon_i &\sim \mathcal{N}(0, \sigma_i^2) \end{aligned} \quad (3)$$

A common assumption is that the causal relationships between η and X_i are linear. In this case, it is possible to write the following Equation system 4 [44, 45].

$$\begin{aligned} X_1 &= \lambda_1 \eta + \varepsilon_1 \\ X_2 &= \lambda_2 \eta + \varepsilon_2 \end{aligned} \quad (4)$$

λ_1 and λ_2 are called the *factor loadings* and represent the correlations of X_1 and X_2 with η [50]. Given that our hypothesis is that η and X_i are standard normal random variables, and that ε_i is distributed normally with a mean equal to 0 and variance σ_i^2 , by calculating the variance of both sides of the equations in Equation system 4, it is possible to derive that $\sigma_i^2 = (1 - \lambda_i^2), i = 1, 2$.

Now, to correctly express X_1 and X_2 as functions of η , we need to define λ_1, λ_2 and σ_1^2, σ_2^2 . According to *path analysis* theory, the correlation between X_1 and X_2 can be expressed as $\rho_{12} = \lambda_1 \cdot \lambda_2$ [44]. With the hypotheses that $\rho_{12} > 0$

Table 1: Assumptions for the use of the latent variable approach

Assumptions ^a
Only two correlated input factors X_1 and X_2
A linear correlation between X_1 and X_2
$\eta, \varepsilon_1, \varepsilon_2, X_1, X_2$ normally distributed as in Equation 3
Linear relation between η and X_1, X_2 , as in Equation 4
Same relation between X_1, X_2 and η , thus $ \lambda_1 = \lambda_2 = \lambda $ in Equation 4
^a X_1, X_2 are the dependent input factors
η is the latent variable
$\varepsilon_1, \varepsilon_2$ are the unique variances

and that X_1 and X_2 have the same relationship with η , thus $\lambda_1 = \lambda_2 = \lambda$, it is possible to define λ as in Equation 5 [44].

$$\lambda = \sqrt{\rho_{12}} \quad (5)$$

Another possible solution is $\lambda = -\sqrt{\rho_{12}}$, where the latent variable has a negative correlation with both X_1 and X_2 . In case of $\rho_{12} < 0$, the absolute values of both factors loadings are equal to $\sqrt{\rho_{12}}$, while their signs are opposite.

According to Equation 4, λ^2 is the portion of the variance of X_i that is attributed to the latent factor. With our approach, λ^2 is the average variance extracted (AVE). AVE can be defined as ‘*the average amount of variation that a latent construct is able to explain in the observed variables*’ [50]. Intuitively, this is the overall amount of variance that ‘is taken’ from our dependent factors X_i and attributed to the latent variable η , in order to define the causal relationships in Equation 4. The general AVE expression, corresponding to one latent variable and k unique variances, is reported in Equation 6 [51]. Considering that $\sigma_i^2 = 1 - \lambda_i^2$, AVE can be calculated as the average of the squares of the factor loadings associated with the latent variable [50].

$$AVE = \frac{\sum_{i=1}^k \lambda_i^2}{\sum_{i=1}^k \lambda_i^2 + \sum_{i=1}^k \sigma_i^2} = \frac{1}{k} \sum_{i=1}^k \lambda_i^2 \quad (6)$$

Considering that in our case $k = 2$ (two dependent factors) and $\lambda_1 \cdot \lambda_2 = \rho$, we can derive the expression in Equation 7.

$$AVE = \frac{1}{2}(\lambda_1^2 + \lambda_2^2) = \frac{1}{2} \left(\lambda_1^2 + \frac{\rho_{12}^2}{\lambda_1^2} \right) \quad (7)$$

If we calculate the first derivative of AVE over λ_1 and set it equal to zero, we can obtain the following expression in Equation 8.

$$\begin{aligned} \frac{dAVE}{d\lambda_1} &= \lambda_1 - \frac{\rho_{12}^2}{\lambda_1^3} = 0 \\ \lambda_1 &= \sqrt{|\rho_{12}|} \\ \lambda_2 &= \text{sign}(\rho_{12}) \cdot \sqrt{|\rho_{12}|} \end{aligned} \quad (8)$$

Where, $\text{sign}(\rho_{12})$ is equal to +1 if $\rho_{12} > 0$, while it is equal to -1 if $\rho_{12} < 0$. If we calculate the second derivative we can see that it is always positive, thus $|\lambda_1| = |\lambda_2|$ corresponds to a minimum. With our hypothesis that X_1 and X_2 have the same relationship with η , the AVE is minimised. This means that we are explaining the correlation between two observed variables by attributing (on average) the minimum variance possible to the latent construct.

With the latent variable approach, instead of two correlated random variables (X_1 and X_2), three independent random variables (η, ε_1 and ε_2) will be considered in the variance-based GSA. In this context, the impact of ε_1 and ε_2 on the model output can be uniquely attributed to X_1 and X_2 , respectively. Instead, it would be impossible to distinguish if the impact of η on the model output is primarily mediated by X_1 or X_2 .

For simplicity, we have considered standardised variables. However, the latent variable approach can easily be extended to data in original units with the use of simple transformations. Nevertheless, in order to use this method several assumptions must be satisfied (summarised in Table 1) and some limitations still exist. The sums of the random variables representing the latent and independent variances must follow the distributions of X_i . This condition is satisfied if both the parameters are normally distributed and it can easily be extended to the case of the two parameters being log-normally distributed (although in this case $\log(X_1)$ and $\log(X_2)$ must be linearly correlated). However, the condition in Equation system 4 is not easily satisfied for other types of distributions. The method presented here is valid when considering two correlated factors and it can be extended to three mutually correlated factors, by using the so

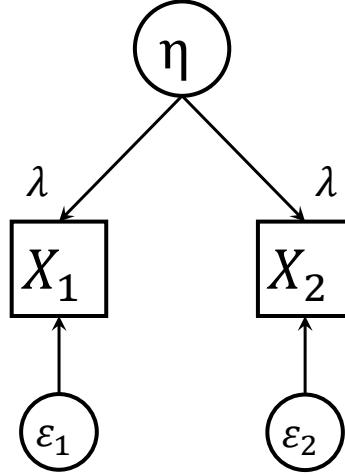


Figure 1: Relationship between the observed, common and unique variances for two correlated parameters and one latent variable. X_1 and X_2 are the observed variables, η is the latent variable, ε_1 and ε_2 are the unique variances and λ are the factor loadings.

called *method of triads* to derive a unique solution for the factor loadings [44]. However, it is possible that there is no unique solution when more than three mutually correlated factors are considered [44]. In this situation, the application of the latent variable approach for GSA would become more challenging.

2.3 Algebraic models

The latent variable approach was initially tested on three algebraic models, namely model 1, 2 and 3, in Equations 9, 10 and 11 respectively.

$$Y = X_1 + X_2 + X_2 \cdot X_3 \quad (9)$$

$$Y = X_1 + X_2 + X_1 \cdot X_3 \quad (10)$$

$$Y = X_1 + X_2 + X_3 + X_4 \quad (11)$$

For all the models, all factors were considered to be normally distributed with means equal to 0 and variances equal to 1, $X_i \sim \mathcal{N}(0, 1)$, $i = 1, 2, 3, 4$. X_1 and X_4 were considered linearly correlated, with a Pearson correlation coefficient of ρ_{14} . Model 1 and model 2 differ in the fact that in model 1, X_1 is not involved in any interaction, while in model 2, X_1 interacts with X_3 .

X_4 does not appear in the model 1 or model 2 equations, consequently, its ‘causal impact’¹ on the model output Y must be null. Intuitively, for both model 1 and 2, the results of a variance-based GSA in absence of correlation, considering only X_1 , X_2 and X_3 , will correctly reflect the structure of the model.

2.4 Whole-body PBPK model for midazolam

A whole-body PBPK model was developed, describing the pharmacokinetics of the drug MDZ following an intravenous (IV) bolus injection in a population of human healthy subjects. The model is represented in Figure 2. This section provides a brief description of the model. For a detailed account of the model equations, the parameters used for the PBPK construction and the algorithm used for generating the population, see the Supplementary Material.

The typical equation used to describe the mass balance in a given organ or tissue t within a PBPK model is reported in Equation 15. For a detailed description and the underlying theories of this model, called *well-stirred perfusion-limited* PBPK, please refer to [52].

$$\frac{dx_t}{dt} = Q_t \left(\frac{x_{art}}{V_{art}} - \frac{x_t/V_t}{P_{t:p}/B : P} \right) \quad (12)$$

Equation 15 is valid for all organs and tissues except the liver, the lungs, the arterial and venous blood. x_t is the drug amount in compartment t , while V_t is the volume. Subscript *art* stands for arterial blood. Q_t is the blood flow to compartment t . $B : P$ is the blood-to-plasma ratio and $P_{t:p}$ is the tissue-to-plasma partition coefficient.

¹Here we refer to ‘causal impact’ as the impact of an input factor X_i on the model output Y that is not due to the dependence of X_i with other factors.

MDZ is primarily metabolised in the liver by the two enzymes, CYP3A4 and CYP3A5. For MDZ both enzymes catalyse two reactions, leading to the formation of two metabolites, *1-hydroxy midazolam* (1-OH-MDZ) and *4-hydroxy midazolam* (4-OH-MDZ) [53, 46]. For this reason, two mass flows corresponding to MDZ metabolism leave the PBPK system from the liver compartment, as represented in Equation system 18.

$$\frac{dx_{liv}}{dt} = Q_{liv} \left(\frac{x_{art}}{V_{art}} - \frac{x_{liv}/V_{liv}}{P_{liv:p}/B:P} \right) + \sum_{t \in S} \left[Q_t \left(\frac{x_t/V_t}{P_{t:p}/B:P} \right) \right] - MET_{3A4} - MET_{3A5} \quad (13)$$

Subscript *liv* stands for liver, *S* represents the splanchnic organs (spleen, pancreas, stomach, small and large intestine). $c_{u,liv}$ is the unbound liver concentration. MET_{3A4} and MET_{3A5} are the fluxes representing the reactions catalysed by CYP3A4 and CYP3A5. All the chemical reactions are described using *Michaelis-Menten* equations [54]. The *Michaelis-Menten* parameters for MDZ are taken from *in vitro* studies [46] and they are scaled to the *in vivo* context as per [55]. One of the main parameters used for the *in vitro* to *in vivo* scaling is the microsomal protein per gram of liver (*MPPGL*) (see supplementary materials for a detailed description of this process).

The population variability of physiological parameters such as the compartment volumes and blood flow was generated with a simple algorithm having as inputs the sex of the subject, the height and the body mass index (BMI).

To simulate an IV bolus injection of 5 mg of MDZ, the initial condition of the venous blood compartment was set equal to 5, while the remaining compartments were set to equal 0. The *area under the curve* (AUC) of the venous plasma compartment was considered the output of interest for the GSA. The AUC is defined as in Equation 14.

$$AUC = \int_{t_{in}}^{t_{end}} \frac{x_{ven}(\tau)}{V_{ven} \cdot B:P} d\tau \quad (14)$$

t_{in} and t_{end} were set to 0 and $24 \cdot 7 h$, respectively. The AUC is a measure of the cumulative exposure of a drug over time. In PK, AUC is an important metric not only to represent exposure, but also to calculate a number of PK parameters using non-compartmental analysis [56]. The distributions of the model parameters considered in this analysis are reported in Table 2.

Table 2: Variable parameters used for the MDZ PBPK model

Parameters	distribution parameters	distribution type	units	references
sex ^d	0, 1	uniform ^a		
height (male) ^e	176.7 (6.15)	normal ^b	cm	[57]
height (female) ^e	163.3 (5.85)	normal ^b	cm	[57]
BMI ^f	18.5, 24.9	uniform ^a	kg/m ²	[58]
[CYP3A4] ^g	137 (41%)	log-normal ^c	(pmol CYP)/(mg MP)	[59]
[CYP3A5] ^g	103 (65%)	log-normal ^c	(pmol CYP)/(mg MP)	[59]
MPPGL ^h	39.79 (27%)	log-normal ^c	(mg prot)/(g liver)	[60]

^a For distribution parameters, *minimum*, *maximum* of the parameter.

^b For distribution parameters, *mean* (*standard deviation*) of the normal variable.

^c For distribution parameters, *mean* (*CV*) of the log-normal variable.

^d If the extracted value is < 0.5 the subject is female (0), otherwise male (1).

^e height for a 20 years old Italian population

^f Body mass index corresponding to the nutritional status of ‘Normal weight’ according to the World Health Organization

^g CYP abundance per mg of microsomal protein

^h mg of microsomal proteins for gram of liver

2.5 Analysis overview

For the GSA, the following methods were applied to both the algebraic and the PBPK models:

- classical variance-based GSA considering all the parameters uncorrelated;
- variance-based GSA grouping together the two correlated parameters;
- the method developed by Kucherenko for computing the variance-based GSA indices in presence of correlation [37];

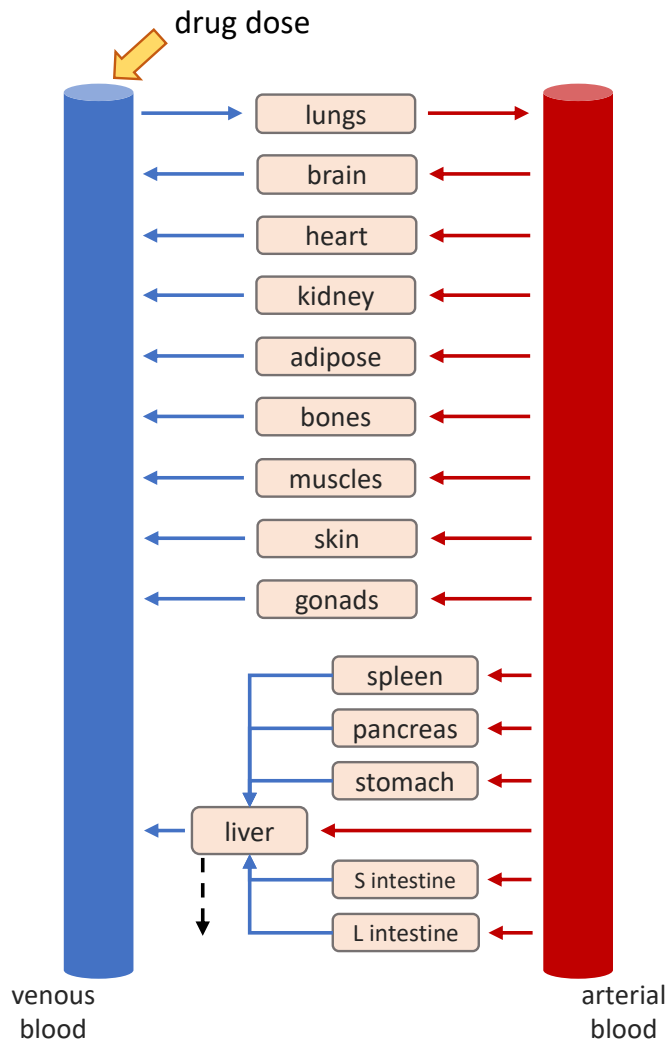


Figure 2: Structure of a general whole-body PBPK model. Each box corresponds to a specific compartment. The red and blue arrows represent the arterial and venous blood flow, respectively. The black-dashed arrow represents elimination through metabolism in the liver. The yellow arrow represent the drug intravenous administration. *S intestine* and *L intestine* are the small and large intestine, respectively.

- the latent variable approach.

Concerning the algebraic models, the analysis was carried out varying ρ_{14} , from -0.9 to 0.9. When $\rho_{14} > 0$, the latent variable was considered to be positively correlated with both X_1 and X_4 ($\lambda > 0$). Instead, when $\rho_{14} < 0$, the latent variable was considered to be positively correlated with X_1 and negatively correlated with X_4 .

For the PBPK model, the (Pearson) correlation between the logarithms of CYP3A4 and CYP3A5 abundances $\rho_{3A4,3A5}$ was considered to equal 0.52, based on proteomic data from human liver samples [61], for the variance-based GSA with grouped factors, for the Kucherenko and the latent variable approaches. In this analysis, all simulated individuals were assumed to express CYP3A5.

All analysis was performed in MATLAB R2020a² [62]. The systems of differential equations were solved with the ode15s MATLAB solver, for a timespan ranging from 0 to $24 \cdot 7$ h. GSA was performed using the software UQLab [63] except for the variance-based GSA with groups, where an 'ad hoc' MATLAB code was developed. For the numerical estimation of the sensitivity indices, within UQLab, the 'homma' estimator was used for the Sobol approach, while the

²The codes are made available at the following link https://github.com/NicolaMelillo/latent_variable_GSA.

default estimator embedded in the software was used for the Kucherenko approach. Concerning the ‘*ad hoc*’ MATLAB code, we used the estimator reported in [28] (the *errata corrige* version). For all the methods, the sample size was fixed to 10,000. The uncertainty of the sensitivity indices estimates was assessed by using 1,000 bootstrap samples, with the exception of the Kucherenko method, where the convergence plots were used.

3 Results

3.1 Algebraic models

The GSA results for the algebraic models 1, 2 and 3, with $\rho_{14} = 0.7$ and $\rho_{14} = 0.9$, are reported in Tables 3, 4 and 5, respectively. In Figure 3 the GSA results obtained with the latent variable and the Kucherenko approaches for the algebraic model 1 are given as a function of ρ_{14} , ranging from -0.9 to 0.9. For the models 2 and 3, the equivalent information is shown in Figure 4 and 5, respectively. Here we begin by reporting the results of model 1 and 2 and then, model 3.

The parameter X_4 does not appear in Equations 9 and 10. Regardless of presence or absence of correlation between X_1 and X_4 its ‘causal’ impact on the output should therefore be null. Hence, intuitively, the results of a variance-based GSA with the classic Sobol’s method considering only X_1 , X_2 and X_3 should be the ones that truly represent the model structure. Any differences in main and total effects for the Kucherenko approach, the latent variable approach and the variance based GSA with grouped factors are therefore due to how these methods handle the correlation.

Concerning the Kucherenko approach, in Figure 3 the higher the absolute value of ρ_{14} is, the higher the main effect of X_4 is, while its total effect always remains equal to 0. This substantially confirms the findings of [32]. Moreover, as the absolute value of the correlation increases, the total effect of X_1 decreases, while the main effect remains stable. From [32] we know that S_1 includes the impact of the correlation of X_1 with X_4 , while $S_{T,1}$ just includes the ‘uncorrelated’ effects. From our example is possible to appreciate that the higher $|\rho_{14}|$ is, the lower the ‘uncorrelated’ effect of X_1 is. In this context it is actually challenging to distinguish between the ‘causal’ effect of X_1 and X_4 on Y and the effect due to their dependence. Similar conclusions can be made for the model 2. By limiting the analysis to the Kucherenko indices, it is challenging to understand how much X_1 is involved in interaction effects and, ultimately, to determine any ranking of importance of the parameters as can be used in practical applications.

Concerning the latent variable approach, presented in Figures 3 and 4, the higher the absolute value of ρ_{14} is, the higher the importance of the latent variable over the unique variances. Ultimately, with ρ_{14} approaching 1 the whole variance of both X_1 and X_4 becomes fully explained by the latent factor and thus, the residual variances’ effect on the output variance tends to 0. Given that the latent variable affects both the correlated factors equally, it is not possible to elucidate if the impact of η on the output variance is primarily mediated by X_1 or X_4 . However, the impact of the unique variances can be uniquely attributed to the correlated factors. In fact, for both models 1 and 2, both the main and total effect of ε_4 are always equal to zero, as seen in Figures 3 and 4. This is unlikely the case for traditional variance-based GSA with groups (see Tables 3 and 4), where, independently of the values of ρ_{14} , it is not possible to determine the impact of the variable within the groups. Notably, if $|\rho|$ is close to 1, the latent variable will fully explain both X_1 and X_4 , resembling the case of the grouping approach. Given that in both the grouping and the latent variable approach we are performing a standard Sobol’s GSA with uncorrelated factors, the interpretation of the sensitivity indices and the factor ranking is straightforward.

In model 1, X_1 is not involved in any interactions. This is discernible when $S_i = S_{T,i}$. In this case, $S_1 = S_{T,1}$, as seen in Table 3 and Figure 4. Neither η or ε_1 are involved in any interactions. This is quite intuitive as the model is linear and X_1 is defined as the sum of the latent variable and the unique variance in the latent variable approach. However, interaction effects between the latent variable and the unique variance will arise, for example, in case of X_1 having a nonlinear effect (e.g., quadratic) on Y^3 . In model 2, X_1 and X_3 show interaction effects, as noted in the Sobol’s GSA results. This happens when $S_{T,i} > S_i$. In Table 4 and Figure 4 we can see that both the latent variable and the unique variance of X_1 show interaction effects.

Concerning model 3, Table 5 and Figure 5, we observe that the sensitivity indices of X_2 and X_3 change in function of ρ_{14} . The traditional variance-based GSA that considers all the factors uncorrelated does not capture this effect. With this simple example, we can see that ignoring the correlation within GSA could potentially bias the overall results of the analysis. Traditional GSA with groups can capture this effect and thus, it can be an easy and reliable method for treating correlations. However, as explained for models 1 and 2, it has the limitation of not distinguishing the impact of the variables within the groups of correlated factors.

Concerning the Kucherenko approach, S_1 and S_4 are close to 0 when ρ_{14} is close to 0 and they both grow as $|\rho_{14}|$ grows. Instead, $S_{T,1}$ and $S_{T,2}$ have almost a parabolic shape. Both the main and total effects of X_1 and X_4 are low for strong negative correlation, probably because in this model the effect of X_1 tends to cancel the one of X_4 on Y and vice versa. For a high positive correlation the total effects tend to zero, while the main effects are close to 0.6.

³If $X_1 = \lambda\eta + \varepsilon$ and $Y = X_1^2$, it is straightforward to derive that $Y = \lambda^2\eta^2 + \varepsilon^2 + 2\lambda\eta\varepsilon$. In this case, there are interaction effects between η and ε .

Regarding the latent variable approach, one interesting observation is that the overall tendency of the unique variances and latent variable sensitivity indices are similar to those of the total and main effects of X_1 and X_4 of the Kucherenko approach, respectively. This probably happens because the unique variances represents the impact of the ‘uncorrelated’ part of the factors, similarly to the total effect of the Kucherenko approach. Instead, both the latent variable and the main effect include the ‘dependent’ part of the factors. However, one important difference is that the latent variable approach is a variance-based GSA performed with independent variables and thus, the indices are easily understandable, this is unlikely the case for the Kucherenko approach. Finally, it is interesting to observe that for negative correlations the impact of the latent variable is zero. This happens because the factor loadings (λ) are equal in module, but opposite in sign and thus, the latent variable term is cancelled from Equation 11.

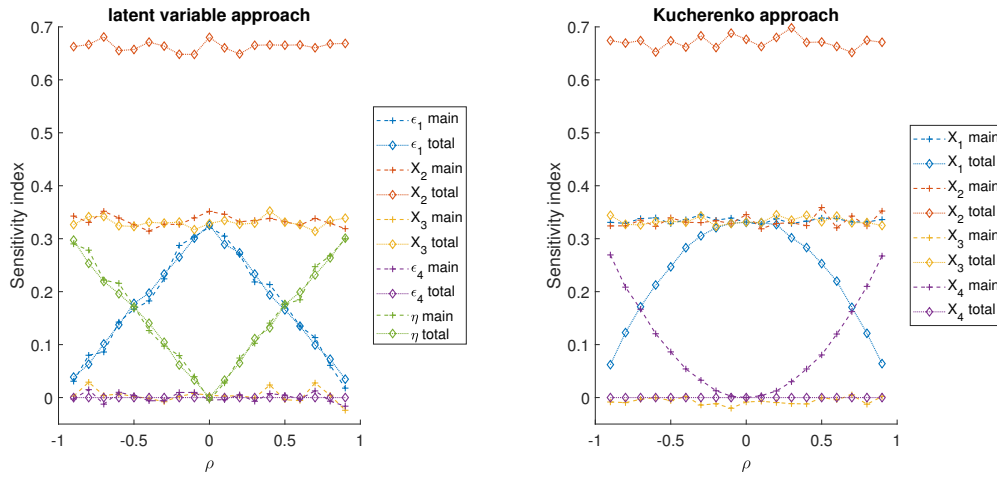


Figure 3: Algebraic model 1 GSA results of the latent variable and the method presented by Kucherenko 2012 [37].

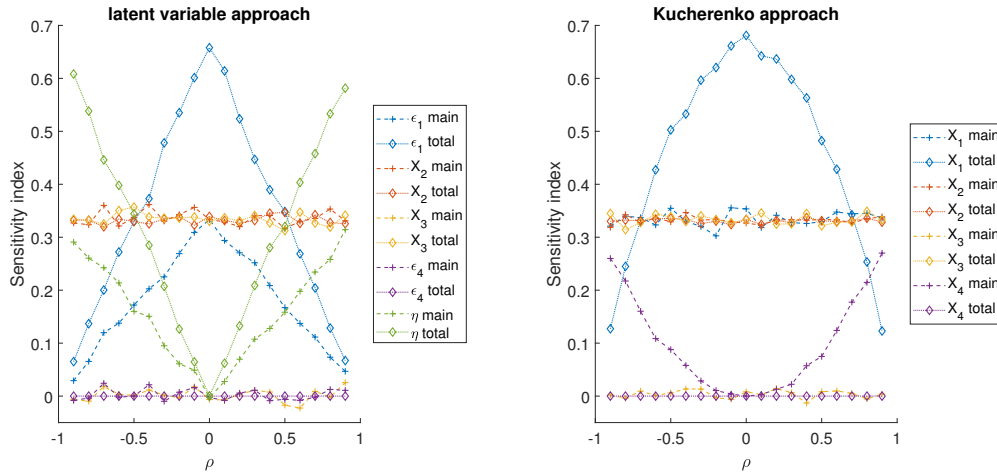


Figure 4: Algebraic model 2 GSA results of the latent variable and the method presented by Kucherenko 2012 [37].

3.2 Whole-body PBPK model for midazolam

The simulated MDZ plasma concentration-time profiles and AUCs for a population of 10,000 subjects are shown in Figures 6 and 7, respectively. The GSA results of Sobol’s method without accounting for the correlation, of the Kucherenko method, of the traditional variance-based GSA with groups and of the latent variable approach are presented in Table 6.

According to the results from Sobol’s GSA, the most important parameters in explaining the variability in AUC are (in order of importance) the MPPGL, CYP3A4 and CYP3A5 abundances. These factors are important because they control the rate of metabolism in the liver. The fact that the metabolism-related parameters are the most important for explaining variability in AUC suggests that the rate-limiting step of drug elimination is the metabolism and not, for

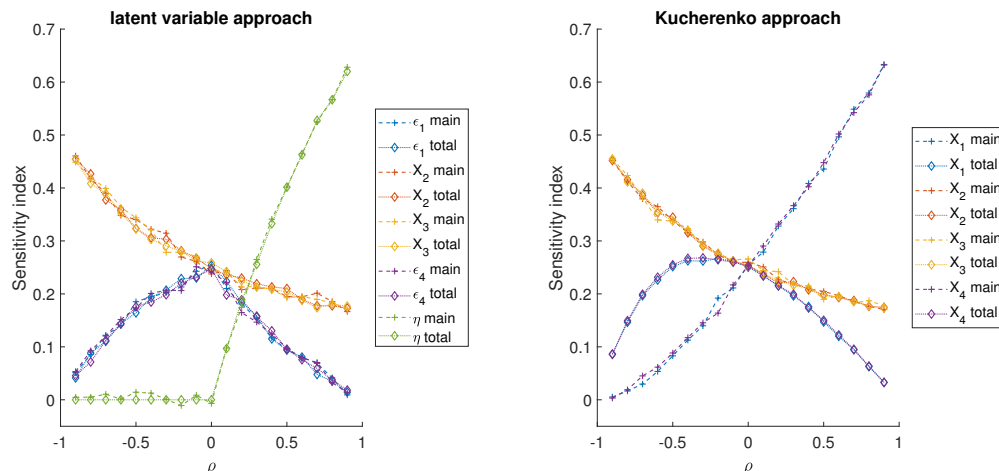


Figure 5: Algebraic model 3 GSA results of the latent variable and the method presented by Kucherenko 2012 [37].

example, liver blood flow. Given that exposure drives drug effect, the interindividual variability in efficacy, due to PK, is mainly explained by genetics in this case example. However, we need to consider that our population is composed by healthy adults with a BMI corresponding to the nutritional status of ‘normal weight’ [58]. The inclusion of overweight or obese subjects may impact the results of the GSA.

Concerning the GSA results obtained with the Kucherenko, the variance-based GSA with groups and the latent variable approach, the sensitivity indices of MPPGL are slightly reduced as compared to Sobol’s GSA. This is most likely related with the fact that the correlation between CYP3A4 and CYP3A5 tends to generate more ‘extreme’ individuals, *i.e.*, poor metabolisers (with low CYP3A4 and low CYP3A5 abundances) and rapid metabolisers (with high CYP3A4 and high CYP3A5 abundances). Thus, as it is possible to observe in Figure 7, the AUC distribution in case of correlation is slightly wider with respect to the case of no correlation. These results are in agreement with our previous studies [4].

Concerning the Kucherenko analysis, it is difficult to confidently use either the main or the total effects for the purpose of factor ranking. For example, by observing the main effect the two most important parameters are CYP3A4 and CYP3A5 abundances. However, it is difficult to understand what the contributions of the variables themselves are and what is due to the correlation. For this reason, in our example, there is a risk of overestimating the importance of the enzymatic abundances and, by extension, underestimating the importance of the other factors. By using the total effect for the factor ranking, there is instead the risk of underestimating the importance of the correlated factors and overestimating the importance of the remaining inputs, as the total effects for the factors involved in the correlation tend to 0 as $|\rho| \rightarrow 1$ [37]. Moreover, by using these two indices, given that for both CYP3A4 and CYP3A5 abundances the total effect is lower than the main effect, it is difficult to understand the effect of interactions.

In the latent variable approach, the factor ranking can be done by examining either the main or at the total effects. This is possible because the correlation between CYP3A4 and CYP3A5 was expressed in terms of a functional relationship between three independent factors, the latent variable and two independent variabilities. Thus, the classical variance-based GSA was used. With this approach, the most important factor in explaining the AUC is η , followed by MPPGL and the independent components of CYP3A4 and CYP3A5. By using either the main or the total effect for the factor ranking, we can confidently assess that the main drivers for the plasma AUC are the metabolism-related parameters. Moreover, with this method it is possible to appreciate the interaction effects, that in this case are mild and do not have a great impact on the factor ranking. A downside of this approach is that η drives both CYP3A4 and CYP3A5 variability. For this reason, given that the latent variable is one of the two most important parameters, it is not possible to appreciate if its importance is primarily caused by the CYP3A4 or CYP3A5 mediated pathway. By investigating the independent components of CYP3A4 and CYP3A5 abundances, it is noted that they do have a similar impact. Intuitively, if one of the two factors was not important for the AUC, the independent component would be equal to zero (however, it is not necessarily true for the opposite case).

The results of the PBPK simulations presented here aim to illustrate a GSA methodology, only. Therefore, we do not recommend their use for other purposes.

Table 3: Results for the algebraic model 1

Factor	Sobol ^a		Kucherenko ^b		Latent variable ^a		Grouped ^a	
	main	total	main	total	main	total	main	total
$\rho_{14} = 0.7$								
X_1^c	0.34 (0.32,0.36)	0.33 (0.31,0.34)	0.33	0.17	0.11 (0.09,0.13)	0.1 (0.9,0.11)	0.31 ^d (0.29,0.33)	0.34 ^d (0.31,0.37)
X_2	0.33 (0.31,0.35)	0.67 (0.64,0.7)	0.32	0.64	0.32 (0.3,0.35)	0.65 (0.63,0.67)	0.31 (0.28,0.33)	0.7 (0.67,0.72)
X_3	0 (-0.03,0.02)	0.33 (0.31,0.35)	0	0.34	0.02 (-0.01,0.04)	0.33 (0.31,0.35)	-0.03 (-0.06,0)	0.32 (0.29,0.34)
X_4^c	0 (-0.02,0.02)	0 (0,0)	0.16	0	0.02 (0,0.03)	0 (0,0)		
η					0.26 (0.24,0.28)	0.23 (0.22,0.25)		
$\rho_{14} = 0.9$								
X_1^c	0.33 (0.31,0.35)	0.35 (0.33,0.37)	0.33	0.06	0.05 (0.03,0.07)	0.04 (0.03,0.04)	0.33 ^d (0.31,0.35)	0.34 ^d (0.31,0.37)
X_2	0.32 (0.29,0.34)	0.66 (0.64,0.69)	0.33	0.69	0.33 (0.31,0.35)	0.65 (0.63,0.68)	0.35 (0.33,0.38)	0.67 (0.64,0.7)
X_3	-0.01 (-0.04,0.02)	0.33 (0.31,0.36)	-0.01	0.35	0.02 (-0.01,0.04)	0.35 (0.33,0.37)	0 (-0.03,0.02)	0.33 (0.31,0.36)
X_4^c	-0.01 (-0.03,0.01)	0 (0,0)	0.27	0	0.01 (-0.01,0.03)	0 (0,0)		
η					0.3 (0.28,0.32)	0.29 (0.27,0.3)		

^a values reported in the table are mean (2.5,97.5) percentiles calculated with 1000 bootstrap samples

^b convergence plots are shown in the supplementary materials

^c for the latent variable model, this refers to the unique variance

^d this refers to the X_1 and X_4 group

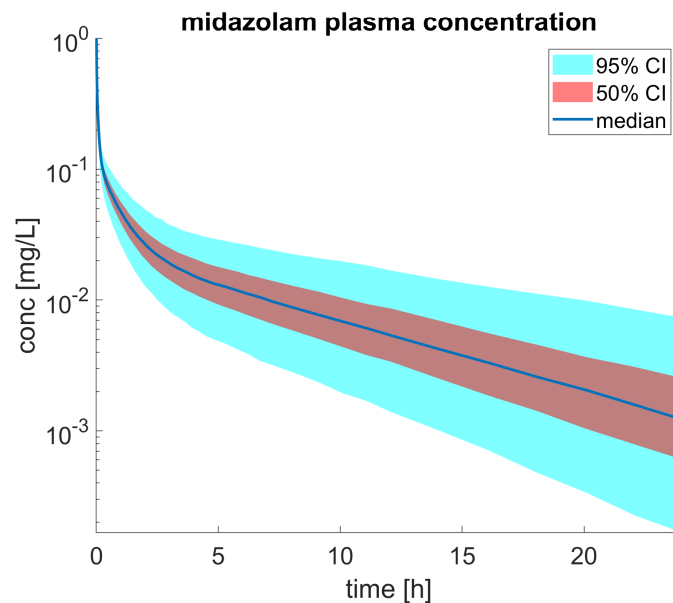


Figure 6: Simulated population midazolam plasma concentration over time following an intravenous (IV) bolus dose of 5 mg. The simulation was performed with the PBPK model for 10,000 individuals. The physiological correlation was considered between the abundances of CYP3A4 and CYP3A5.

Table 4: Results for the algebraic model 2

Factor	Sobol ^a		Kucherenko ^b		Latent variable ^a		Grouped ^a	
	main	total	main	total	main	total	main	total
$\rho_{14} = 0.7$								
X_1^c	0.34 (0.32,0.36)	0.68 (0.66,0.71)	0.32	0.34	0.11 (0.09,0.13)	0.2 (0.18,0.21)	0.33 ^d (0.3,0.35)	0.68 ^d (0.65,0.71)
X_2	0.32 (0.3,0.34)	0.33 (0.32,0.35)	0.33	0.32	0.33 (0.31,0.35)	0.33 (0.31,0.35)	0.32 (0.3,0.34)	0.34 (0.31,0.37)
X_3	0 (-0.02,0.03)	0.34 (0.32,0.36)	0	0.34	0.01 (-0.01,0.04)	0.33 (0.3,0.35)	-0.03 (-0.05,-0.01)	0.33 (0.31,0.35)
X_4^c	-0.01 (-0.03,0.01)	0 (0,0)	0.16	0	0.01 (-0.01,0.02)	0 (0,0)		
η					0.24 (0.22,0.26)	0.47 (0.45,0.49)		
$\rho_{14} = 0.9$								
X_1^c	0.33 (0.31,0.35)	0.66 (0.63,0.69)	0.32	0.13	0.03 (0.01,0.05)	0.06 (0.05,0.07)	0.36 ^d (0.33,0.38)	0.65 ^d (0.62,0.68)
X_2	0.32 (0.3,0.34)	0.34 (0.32,0.35)	0.32	0.33	0.32 (0.3,0.34)	0.33 (0.32,0.35)	0.35 (0.33,0.37)	0.32 (0.29,0.35)
X_3	0 (-0.03,0.03)	0.34 (0.32,0.37)	0	0.35	-0.01 (-0.03,0.01)	0.34 (0.32,0.37)	0.01 (-0.01,0.04)	0.34 (0.32,0.37)
X_4^c	0 (-0.02,0.02)	0 (0,0)	0.25	0	0 (-0.02,0.02)	0 (0,0)		
η					0.29 (0.27,0.32)	0.61 (0.59,0.64)		

^a values reported in the table are mean (2.5,97.5) percentiles calculated with 1000 bootstrap samples

^b convergence plots are shown in the supplementary materials

^c for the latent variable model, this refers to the unique variance

^d this refers to the X_1 and X_4 group

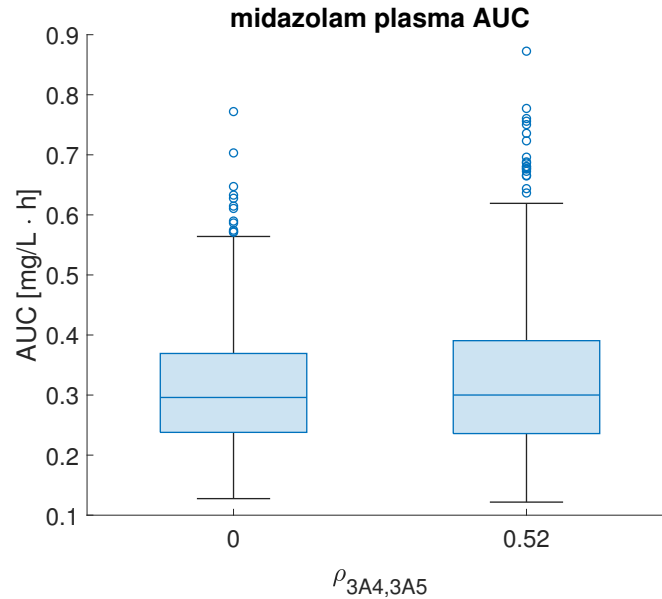


Figure 7: Simulated midazolam AUC distribution both in presence and absence of correlation between CYP3A4 and CYP3A5 abundances. The simulation was performed with the PBPK model for 10,000 individuals.

Table 5: Results for the algebraic model 3

Factor	Sobol ^a		Kucherenko ^b		Latent variable ^a		Grouped ^a	
	main	total	main	total	main	total	main	total
$\rho_{14} = 0.7$								
X_1^c	0.25 (0.23,0.26)	0.25 (0.23,0.26)	0.55	0.1	0.07 (0.05,0.09)	0.05 (0.04,0.06)	0.62 ^d (0.6,0.64)	0.63 ^d (0.61,0.65)
X_2	0.25 (0.23,0.26)	0.24 (0.23,0.26)	0.19	0.19	0.18 (0.16,0.2)	0.19 (0.18,0.2)	0.19 (0.17,0.21)	0.18 (0.16,0.2)
X_3	0.26 (0.24,0.27)	0.25 (0.24,0.27)	0.18	0.19	0.2 (0.18,0.22)	0.19 (0.18,0.2)	0.18 (0.16,0.2)	0.19 (0.17,0.2)
X_4^c	0.26 (0.24,0.28)	0.25 (0.24,0.27)	0.54	0.1	0.06 (0.04,0.08)	0.05 (0.05,0.06)		
η					0.51 (0.49,0.53)	0.51 (0.49,0.53)		
$\rho_{14} = 0.9$								
X_1^c	0.24 (0.22,0.26)	0.25 (0.24,0.26)	0.63	0.03	0.02 (0,0.04)	0.02 (0.02,0.02)	0.65 ^d (0.63,0.67)	0.65 ^d (0.63,0.67)
X_2	0.24 (0.22,0.26)	0.25 (0.24,0.26)	0.17	0.17	0.18 (0.16,0.2)	0.17 (0.16,0.18)	0.17 (0.15,0.19)	0.17 (0.15,0.19)
X_3	0.26 (0.24,0.28)	0.24 (0.23,0.25)	0.18	0.17	0.17 (0.15,0.19)	0.17 (0.16,0.18)	0.18 (0.16,0.2)	0.19 (0.17,0.21)
X_4^c	0.25 (0.23,0.27)	0.26 (0.25,0.28)	0.62	0.03	0.02 (0,0.04)	0.02 (0.01,0.02)		
η					0.63 (0.61,0.64)	0.62 (0.6,0.64)		

^a values reported in the table are mean (2.5,97.5) percentiles calculated with 1000 bootstrap samples

^b convergence plots are shown in the supplementary materials

^c for the latent variable model, this refers to the unique variance

^d this refers to the X_1 and X_4 group

Table 6: GSA results for the MDZ PBPK model

Factor	Sobol ^a		Kucherenko ^b		Latent variable ^a		Grouped ^a	
	main	total	main	total	main	total	main	total
	$\rho_{3A4,3A5} = 0.52$							
sex	0 (-0.02,0.02)	0.02 (0.01,0.03)	0.01	0.02	0.03 (0.01,0.05)	0.02 (0.01,0.02)	0 (-0.02,0.02)	0.01 (-0.03,0.04)
height	0.01 (-0.01,0.03)	0.05 (0.04,0.05)	0.02	0.03	0.04 (0.02,0.06)	0.03 (0.02,0.04)	0.01 (-0.01,0.03)	0.01 (-0.02,0.05)
BMI	0.03 (0.01,0.05)	0.05 (0.04,0.06)	0.03	0.03	0.04 (0.02,0.07)	0.03 (0.02,0.05)	0.01 (-0.01,0.03)	0.03 (-0.01,0.06)
MPPGL	0.29 (0.27,0.31)	0.39 (0.37,0.41)	0.25	0.3	0.26 (0.24,0.29)	0.3 (0.27,0.32)	0.24 (0.22,0.27)	0.29 (0.26,0.32)
CYP3A4 ^c	0.27 (0.25,0.3)	0.33 (0.31,0.35)	0.49	0.22	0.12 (0.1,0.15)	0.15 (0.13,0.17)	0.61 ^b (0.58,0.64)	0.69 ^d (0.67,0.72)
CYP3A5 ^c	0.23 (0.2,0.25)	0.29 (0.27,0.31)	0.42	0.15	0.09 (0.07,0.09)	0.1 (0.09,0.12)		
η					0.43 (0.41,0.46)	0.48 (0.46-0.5)		

^a values reported in the table are mean (2.5,97.5) percentiles calculated with 1000 bootstrap samples

^b convergence plots are shown in the supplementary materials

^c for the latent variable model, this refers to the unique variance

^d refers to the group of CYP3A4 and CYP3A5

4 Discussion

GSA is gaining use in modelling for pharmaceuticals, especially in the field of PBPK M&S. Recent applications in the literature [3, 4, 5, 6, 7, 8, 9, 31] and regulatory discussions [1, 2] have indicated the usefulness of these methods and it is likely that GSA will become an important feature of modelling in pharmaceutical R&D and for regulatory decision-making. This development is welcomed, indeed in the field of toxicology GSA is an important part of best practices for risk assessment of dose metric predictions [6, 64, 65].

In order for GSA to gain wider use, the issues of usability and interpretation of the results need to be considered. PBPK M&S is an interdisciplinary effort highly reliant on experts in several domains, including medicinal chemistry, *in vitro* drug metabolism, pharmacokinetics, pharmacology, toxicology, statistical and mathematical modelling, and more. Further, modelling activities are an important tool for supporting a wide variety of decisions in R&D and regulatory submissions. For this reason, dedicated user-friendly software platforms are widely used, facilitating standardisation and easy access for non-expert users. We suspect that this is likely to hold true across many different domains, and therefore relevant across areas of application. In this context, particular attention in communicating GSA results should be paid.

Most whole-body PBPK models include several sets of correlated parameters, many of which constrain the models to realistic parameter combinations. It is therefore important that these correlations are accounted for when performing GSA. Several GSA methodologies have been proposed to account for dependent inputs [37, 36, 38, 32, 33] and the method developed by Kucherenko was applied to PBPK models and implemented in a recent version of one of the most widely used PBPK software platforms in pharmaceutical industry [10, 39]. However, considerable debate is still ongoing amongst GSA practitioners on how to appropriately interpret the outcomes of these methods. We believe that the use of methodologies whose interpretation is still a matter of debate, require appropriate care in cases where GSA is called upon to support critical decisions, such as those relating to patient safety.

In this work, we propose a relatively simple method using a latent variable approach that deals with correlated input variables in variance-based GSA. The method expresses the correlation between two factors as causal relationships between a latent factor, η , and two unique variances. As a result this allows the use of classical Sobol's GSA with uncorrelated factors. In our opinion, the approach provides an intuitive process for implementation and interpretation as illustrated in the analysis for MDZ. By ranking the factors according to the total effects of Sobol's GSA, it was possible to clearly interpret the sensitivity indices. This allows insights into the model behaviour and to understand what the main drivers of variability are in a given output. By having a unique, easy and universally recognised interpretation of the sensitivity indices, it is possible to use GSA for supporting decision-making with increased confidence.

One of several alternatives to the latent variable approach would be the use of traditional variance-based GSA with groups. The main advantage is that this method allows treating more than two, or three, dependent factors and other dependencies than the linear correlations. However, as highlighted in the results section, with this approach is not possible to separately distinguish the impact of the dependent variables within a given group. Another alternative could be to assign a unidirectional dependency between the two correlated factors as we have done in a previous study in the context of PBPK models [4]. However, by doing so to describe the dependency, this will affect the relative significance of one input over the other. The potentially arbitrary choice of assigning dependency will increase the importance of the independent variable in the GSA and may produce misleading results. With the latent variable approach we renounce any attempt to completely distinguish the impact of the two correlated inputs on a given model output. Instead, we highlight the impact of the latent variable η (as the 'common cause') along with the independent part.

Here we also attempt to examine the shortcomings of the latent variable approach. In fact, the method presents some limitations with regards to the number and the distribution of the factors that are mutually correlated, as described in section 2. Moreover, the results of the latent variable approach need to be interpreted in light of the assumptions summarised in Table 1. In case one or more of these assumption are not satisfied, the use of traditional GSA with groups is likely a better choice. Despite this, we believe that the latent variable approach can be of use. This would be true at least until further research is done and a clear, universally recognised interpretation of the sensitivity indices have been agreed for more general GSA methods for dependent inputs that rely on fewer assumptions, such as the approaches proposed by Kucherenko *et al.* [37] and Mara *et al.* [32].

5 Declaration of Interest

None.

6 Acknowledgements

We would like to thank Professor Paolo Magni of Università degli Studi di Pavia for valuable discussions and suggestions. This research did not receive any specific grant from funding agencies in the public, commercial, or not-for-profit sectors.

A Physiologically based pharmacokinetic (PBPK) model for midazolam

The typical equation used to describe the mass balance in a given organ or tissue t within a physiologically based pharmacokinetic (PBPK) model is reported in Equation 15.

$$\frac{dx_t}{dt} = Q_t \left(\frac{x_{art}}{V_{art}} - \frac{x_t/V_t}{P_{t:p}/B : P} \right) \quad (15)$$

Equation 15 is valid for all organs or tissues except the liver, the lungs, the arterial and venous blood. x_t is the drug amount in compartment t , while V_t is the volume. Subscript art denotes arterial blood. Q_t is the blood flow to compartment t . $B : P$ is the blood-to-plasma ratio, that is an experimentally derived parameter representing the whole blood drug concentration, divided by the plasma drug concentration at steady state. $P_{t:p}$ is the tissue-to-plasma partition coefficient and represents the tissue drug concentration divided by the plasma drug concentration at steady state. Given the challenges in the experimental measurements of this parameter, several semi-empirical models have been developed over the years, describing $P_{t:p}$ as a function of drug and tissue properties [66]. In this work, the Berezhkovskiy model, given in Equation 16, was used [67]:

$$P_{t:p} = \frac{D_{v,ow} \cdot (V_{nl,t} + 0.3 \cdot V_{ph,t}) + (V_{w,t}/fu_t + 0.7 \cdot V_{ph,t})}{D_{v,ow} \cdot (V_{nl,p} + 0.3 \cdot V_{ph,p}) + (V_{w,p}/fu_p + 0.7 \cdot V_{ph,p})} \quad (16)$$

$V_{nl,t}$ and $V_{nl,p}$ are the volume fractions of neutral lipids in tissue and plasma, respectively; $V_{ph,t}$ and $V_{ph,p}$ are the volume fractions of phospholipids in tissue and plasma; $V_{w,t}$ and $V_{w,p}$ are the water volume fractions in tissue and plasma. Volume fractions are reported in Table 7. $D_{v,ow}$ is the drug partition coefficient between vegetable oil and water and it was obtained as follows $\log D_{v,ow} = 1.115 \cdot \log P_{o,w}$, with $\log P_{o,w}$ the octanol to water partition coefficient [68]. fu_p and fu_t are the drug fraction unbound in plasma and tissue, with the latter calculated as: $fu_t = 1/(1 + 0.5 \cdot (1 - fu_p)/fu_p)$ [68]. All the drug related parameters are given in Table 9.

The equations for the lungs, arterial and venous blood are reported in equation system 17.

$$\begin{aligned} \frac{dx_{lungs}}{dt} &= Q_{tot} \left(\frac{x_{ven}}{V_{ven}} - \frac{x_{lungs}/V_{lungs}}{P_{lungs:p}/B : P} \right) \\ \frac{dx_{art}}{dt} &= Q_{tot} \left(\frac{x_{lungs}/V_{lungs}}{P_{lungs:p}/B : P} - \frac{x_{art}}{V_{art}} \right) \\ \frac{dx_{ven}}{dt} &= \sum_{t \in \mathcal{T}} \left[Q_t \left(\frac{x_t/V_t}{P_{t:p}/B : P} \right) \right] - Q_{tot} \cdot \frac{x_{ven}}{V_{ven}} \end{aligned} \quad (17)$$

Subscript ven stands for venous blood. \mathcal{T} represents all the tissues except lungs, arterial and venous blood, small and large intestine, stomach, spleen and pancreas. The difference between lung and Equation 15 is that the lungs receive the input from venous blood with a flux equal to Q_{tot} , or cardiac output. The arterial blood compartment receives its input from the lungs, while the venous blood compartment receives its input from the outputs of all organs defined in \mathcal{T} .

Midazolam (MDZ) is primarily metabolised in the liver by the two enzymes, CYP3A4 and CYP3A5. For MDZ both enzymes catalyse two reactions, leading to the formation of two metabolites, *1-hydroxy midazolam* (1-OH-MDZ) and *4-hydroxy midazolam* (4-OH-MDZ) [53, 46]. For this reason, two mass flows corresponding to MDZ metabolism leave the PBPK system from the liver compartment following intravenous drug administration, as represented in Equation system 18.

$$\begin{aligned} \frac{dx_{liv}}{dt} &= Q_{liv} \left(\frac{x_{art}}{V_{art}} - \frac{x_{liv}/V_{liv}}{P_{liv:p}/B : P} \right) + \sum_{t \in \mathcal{S}} \left[Q_t \left(\frac{x_t/V_t}{P_{t:p}/B : P} \right) \right] \\ &\quad - MET_{3A4} - MET_{3A5} \\ MET_{3A4} &= \frac{\tilde{V}_{max,3A4,1-OH} \cdot c_{u,liv}}{K_{M,3A4,1-OH} + c_{u,liv}} + \frac{\tilde{V}_{max,3A4,4-OH} \cdot c_{u,liv}}{K_{M,3A4,4-OH} + c_{u,liv}} \\ MET_{3A5} &= \frac{\tilde{V}_{max,3A5,1-OH} \cdot c_{u,liv}}{K_{M,3A5,1-OH} + c_{u,liv}} + \frac{\tilde{V}_{max,3A5,4-OH} \cdot c_{u,liv}}{K_{M,3A5,4-OH} + c_{u,liv}} \end{aligned} \quad (18)$$

Subscript liv stands for liver, \mathcal{S} represents the splanchnic organs (spleen, pancreas, stomach, small and large intestine). $c_{u,liv}$ is the unbound liver concentration, equal to $x_{liv} \cdot fu_t/V_{liv}$, where fu_t is the fraction unbound drug in the tissue. MET_{3A4} and MET_{3A5} are the fluxes representing the reactions catalysed by CYP3A4 and CYP3A5. Subscripts $1 - OH$ and $4 - OH$ refer to the reactions leading to the formation of 1-OH-MDZ and 4-OH-MDZ. All the chemical

reactions are described using *Michaelis-Menten* equations [54], where \tilde{V}_{max} is the *in vivo* maximum reaction rate and K_M is the substrate concentration at which the rate is half of \tilde{V}_{max} . \tilde{V}_{max} is function of the *in vivo* enzyme abundance and is derived in equation 19, as per [55].

$$\tilde{V}_{max} = V_{max} \cdot [CYP] \cdot MPPGL \cdot W_{liv} \quad (19)$$

V_{max} is the experimentally determined *in vitro* maximum rate per amount of CYP isoform, in $(pmol/min)/(pmol\ CYP)$. $[CYP]$ is the enzyme amount per amount of microsomal protein⁴ (MP), in $(pmol\ CYP)/(mg\ MP)$. $MPPGL$ is the amount of microsomal protein per gram of liver, in $(mg\ MP)/(g\ liver)$. Finally, W_{liv} is the liver weight in grams.

For simulating the pharmacokinetics in a given population of subjects, the PBPK model parameters, such as organ volumes and blood flows, need to be generated reflecting the population distribution. We developed a simple algorithm for generating the organ volumes and blood flows. Briefly:

1. the sex of the subject is extracted;
2. according to the sex, the mean cardiac output and the parameters for height and body mass index (BMI) distributions are fixed;
3. height and BMI of the subject are extracted;
4. the body weight (BW , in kg) is calculated as $BW = BMI \cdot h^2$, where h is the height in m ;
5. the cardiac output (CO) is calculated as $CO = \left(\frac{h}{h_{mean}}\right)^{0.75} \cdot CO_{mean}$, with h_{mean} and CO_{mean} the subjects' mean height and cardiac output, respectively [69];
6. organ weights and blood flows were derived by multiplying BW and CO for the respective organs fractions, given in Table 8;
7. organs volumes were derived by dividing the organ weights with organ densities, reported in Table 7.

⁴Vesicles derived from the endoplasmic reticulum abundant in drug metabolising enzymes.

B PBPK parameters

Table 7: Organs composition

Organs	neutral lipids fraction [68]	phospholipids fraction [68]	water fraction [68]	organ density ^c
Adipose	0.79	0.002	0.18	0.916
Bone	0.074	0.0011	0.439	1.4303
Brain	0.051	0.0565	0.77	1.0365
Heart	0.0115	0.0166	0.758	1.03
Muscle	0.0238	0.0072	0.76	1.041
Skin	0.0284	0.0111	0.718	1.1754
Spleen	0.0201	0.0198	0.788	1.054
Kidney	0.0207	0.0162	0.783	1.05
Gonads ^a	0.0048	0.01	0.8	1 ^e
Lung	0.003	0.009	0.811	1.0515
Stomach ^b	0.0487	0.0163	0.718	1.046
Small intestine ^b	0.0487	0.0163	0.718	1.046
Large intestine ^b	0.0487	0.0163	0.718	1.046
Liver	0.0348	0.0252	0.751	1.08 ^f
Pancreas	0.0403 ^d	0.009 ^d	0.641 ^d	1.045
Plasma	0.0035	0.00225	0.945	1 ^e

^a Values taken from *Open Systems Pharmacology suite* version 7.1.

^b Values for stomach, small and large intestine were supposed equal.

^c Calculated using specific gravity values from [70], considering that water density is 1 *kg/L*.

^d values taken from [71, 72]

^e Gonads and blood density were fixed to 1.

^f Value taken from [73].

Table 8: Organs weight, blood flows and blood content

Organs	weight fraction ^b		blood flow fraction ^a		blood fraction ^c	
	male	female	male	female	male	female
Adipose	0.2040	0.3220	0.0530	0.0900	0.05	0.0850
Bone	0.1620	0.1520	0.0530	0.0500	0.07	0.07
Brain	0.0210	0.0230	0.1280	0.130	0.012	0.012
Heart	0.0057	0.0055	0.0430	0.05	0.01	0.01
Muscle	0.4430	0.3380	0.1810	0.12	0.14	0.105
Skin	0.0520	0.0450	0.0530	0.05	0.03	0.03
Spleen	0.0033	0.0037	0.0320	0.03	0.014	0.0104
Kidney	0.0060	0.0067	0.2170	0.2	0.02	0.02
Gonads	0.0006	0.0002	0.0005	0.0002	0.0004	0.0002
Lung	0.0180	0.0170	1	1	0.1050	0.1050
Stomach	0.0023	0.0027	0.0110	0.01	0.01	0.01
Small intestine	0.0100	0.0120	0.1060	0.12	0.038	0.038
Large intestine	0.0056	0.0069	0.0430	0.05	0.022	0.022
Liver	0.0320	0.0320	0.0690	0.07	0.1	0.1
Pancreas	0.0026	0.0028	0.0110	0.01	0.006	0.006
Blood	0.0767 ^d	0.0683 ^d	-	-	(0,06,0.18) ^e	(0.06,0.18) ^e

^a Organ weight fraction (including blood content) on total body weight [69].

^b Fraction of cardiac output directed to each organ [69].

^c Fraction of blood weight (relative to total blood weight) [74].

^d Blood fraction on total body weight [74].

^e (arterial fraction, venous fraction) [74].

Table 9: Midazolam related parameters

Parameters	value	units	references
$B : P$	0.66		[75]
$f u_p$	0.0303		[75]
molecular weight	325.77	g/mol	[76]
$\log_{10} P_{ow}$	3.13		[76]
$V_{max,3A4,1}$	1.96	$pmol/min/(pmol CYP)$	[46]
$K_{M,3A4,1}$	2.69	μM	[46]
$V_{max,3A4,4}$	2.52	$pmol/min/(pmol CYP)$	[46]
$K_{M,3A4,4}$	29	μM	[46]
$V_{max,3A5,1}$	6.7	$pmol/min/(pmol CYP)$	[46]
$K_{M,3A5,1}$	10.7	μM	[46]
$V_{max,3A5,4}$	0.52	$pmol/min/(pmol CYP)$	[46]
$K_{M,3A5,4}$	12.1	μM	[46]

C Convergence of the Kucherenko indices

Figures 8 to 14 detail the convergence of the Kucherenko indices for the various models that were examined.

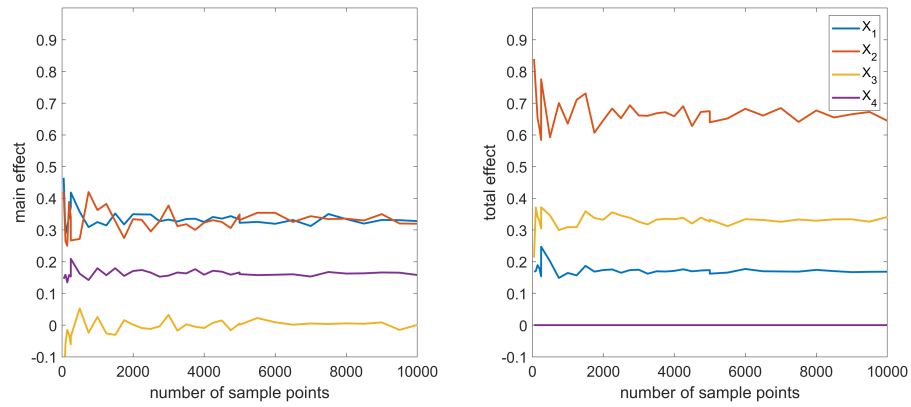


Figure 8: Convergence plot for the Kucherenko indices of the algebraic model 1, with $\rho = 0.7$

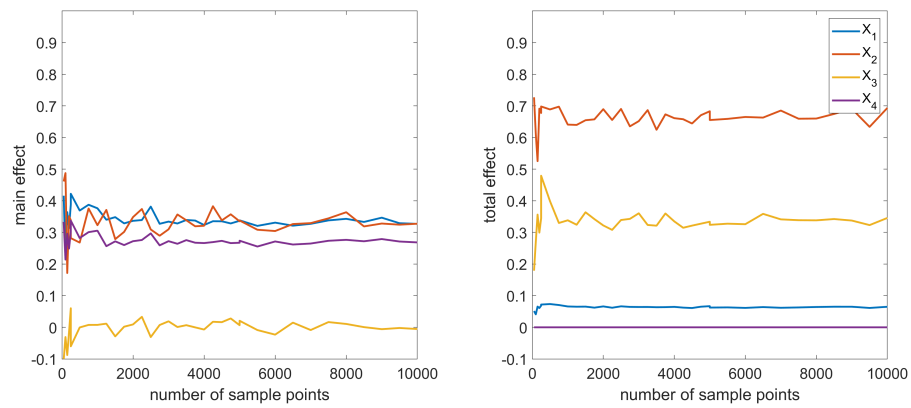


Figure 9: Convergence plot for the Kucherenko indices of the algebraic model 1, with $\rho = 0.9$

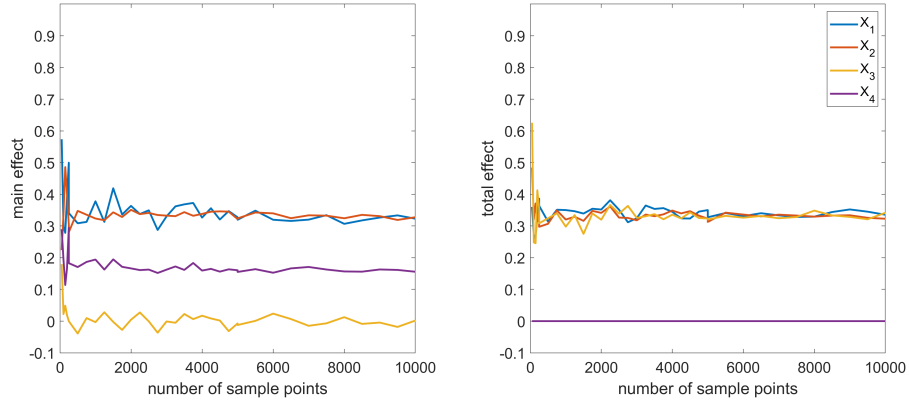


Figure 10: Convergence plot for the Kucherenko indices of the algebraic model 2, with $\rho = 0.7$

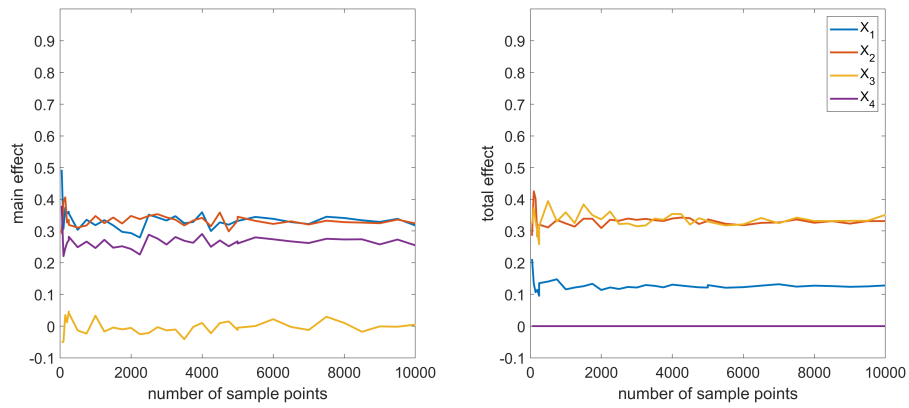


Figure 11: Convergence plot for the Kucherenko indices of the algebraic model 2, with $\rho = 0.9$

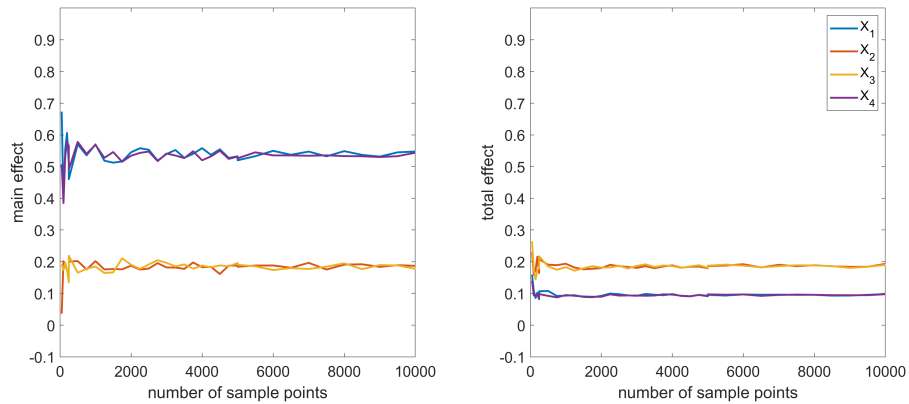


Figure 12: Convergence plot for the Kucherenko indices of the algebraic model 3, with $\rho = 0.7$

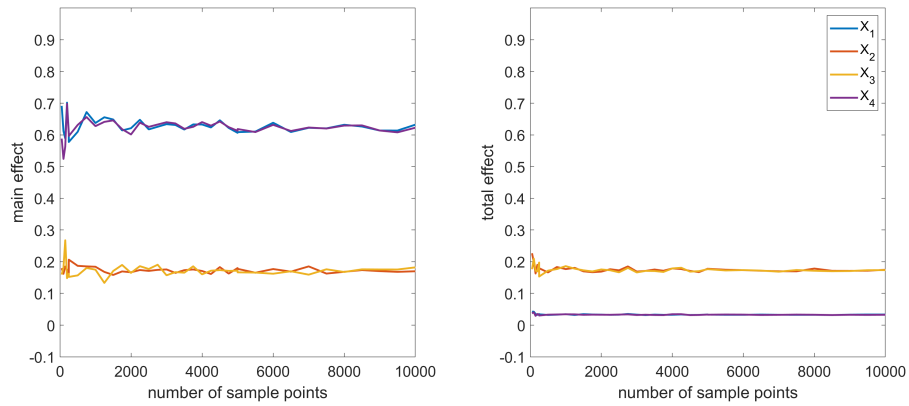


Figure 13: Convergence plot for the Kucherenko indices of the algebraic model 3, with $\rho = 0.9$

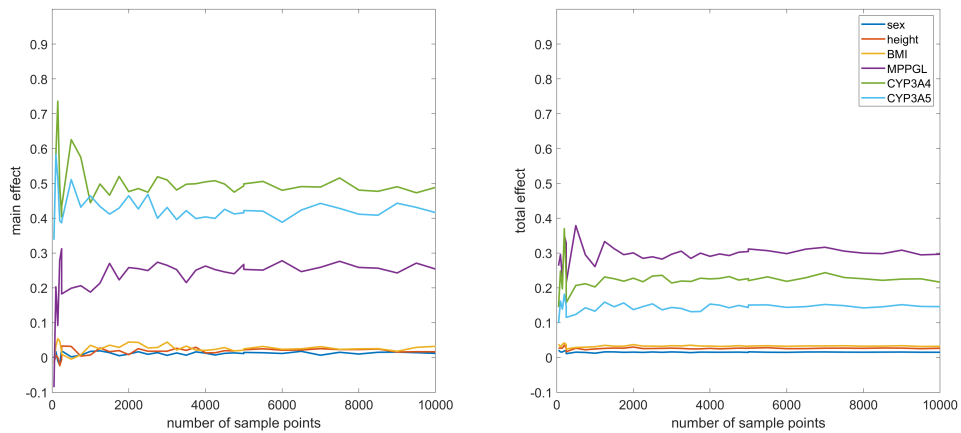


Figure 14: Convergence plot for the Kucherenko indices of the PBPK model for subjects expressing CYP3A5

References

- [1] CHMP (EMA). Guideline on the reporting of physiologically based pharmacokinetic (PBPK) modelling and simulation. Technical Report EMA/CHMP/458101/2016, Committee for Medicinal Products for Human Use (CHMP), European Medicines Agency (EMA), London, UK, December 2018.
- [2] CDER. Physiologically based pharmacokinetic analyses - format and content: Guidance for industry, 2018.
- [3] Nicola Melillo, Leon Aarons, Paolo Magni, and Adam S. Darwich. Variance based global sensitivity analysis of physiologically based pharmacokinetic absorption models for bcs i-iv drugs. *Journal of Pharmacokinetics and Pharmacodynamics*, 46(1):27–42, February 2019.
- [4] Nicola Melillo, Adam S. Darwich, Paolo Magni, and Amin Rostami-Hodjegan. Accounting for inter-correlation between enzyme abundance: a simulation study to assess implications on global sensitivity analysis within physiologically-based pharmacokinetics. *Journal of Pharmacokinetics and Pharmacodynamics*, 46(2):137–154, April 2019.
- [5] Nicola Melillo, Silvia Grandoni, Nicola Cesari, Giandomenico Brogin, Paola Puccini, and Paolo Magni. Inter-compound and Intra-compound Global Sensitivity Analysis of a Physiological Model for Pulmonary Absorption of Inhaled Compounds. *The AAPS Journal*, 22(5):116, August 2020.
- [6] Kevin McNally, Richard Cotton, and George D. Loizou. A Workflow for Global Sensitivity Analysis of PBPK Models. *Frontiers in Pharmacology*, 2:31, 2011.
- [7] X-Y Zhang, Mn Trame, Lj Lesko, and S Schmidt. Sobol Sensitivity Analysis: A Tool to Guide the Development and Evaluation of Systems Pharmacology Models. *CPT: Pharmacometrics & Systems Pharmacology*, 4(2):69–79, February 2015.
- [8] Pankaj R. Daga, Michael B. Bolger, Ian S. Haworth, Robert D. Clark, and Eric J. Martin. Physiologically Based Pharmacokinetic Modeling in Lead Optimization. 2. Rational Bioavailability Design by Global Sensitivity Analysis To Identify Properties Affecting Bioavailability. *Molecular Pharmaceutics*, 15(3):831–839, March 2018.
- [9] E. Yau, A. Olivares-Morales, M. Gertz, N. Parrott, A. S. Darwich, L. Aarons, and K. Ogungbenro. Global sensitivity analysis of the rodgers and rowland model for prediction of tissue: Plasma partitioning coefficients: Assessment of the key physiological and physicochemical factors that determine small-molecule tissue distribution. *AAPS J*, 22(2):41, 2020.
- [10] Dan Liu, Linzhong Li, Amin Rostami-Hodjegan, and Masoud Jamei. Investigating Impacts of Model Parameters Correlations in Global Sensitivity Analysis: Determining the most influential parameters of a Minimal PBPK Model of Midazolam. In *PAGE 28, Abstr 8875 [www.page-meeting.org/?abstract=8875]*, Stockholm, Sweden, 2019.
- [11] EFPIA MID3 Workgroup, SF Marshall, R Burghaus, V Cosson, SYA Cheung, M Chenel, O DellaPasqua, N Frey, B Hamrén, L Harnisch, F Ivanow, T Kerbusch, J Lippert, PA Milligan, S Rohou, A Staab, JL Steimer, C Tornøe, and SAG Visser. Good practices in model-informed drug discovery and development: Practice, application, and documentation. *CPT: Pharmacometrics & Systems Pharmacology*, 5(3):93–122, 2016.
- [12] Andrea Saltelli, Ângela Guimaraes Pereira, Jeroen P. Van der Sluijs, and Silvio Funtowicz. What do I make of your latinorum? Sensitivity auditing of mathematical modelling. *International Journal of Foresight and Innovation Policy*, 9(2/3/4):213, 2013.
- [13] L. Aarons. Physiologically based pharmacokinetic modelling: a sound mechanistic basis is needed. *British Journal of Clinical Pharmacology*, 60(6):581–583, 2005. _eprint: <https://bpspubs.onlinelibrary.wiley.com/doi/pdf/10.1111/j.1365-2125.2005.02560.x>.
- [14] P. L. Bonate. Recommended reading in population pharmacokinetic pharmacodynamics. *AAPS J*, 7(2):E363–73, 2005.
- [15] H. M. Jones and K. Rowland-Yeo. Basic Concepts in Physiologically Based Pharmacokinetic Modeling in Drug Discovery and Development. *CPT: Pharmacometrics & Systems Pharmacology*, page 63, 2013.
- [16] A. F. Sasso, S. S. Isukapalli, and P. G. Georgopoulos. A generalized physiologically-based toxicokinetic modeling system for chemical mixtures containing metals. *Theor Biol Med Model*, 7:17, 2010.
- [17] I. Nestorov. Whole-body physiologically based pharmacokinetic models. *Expert Opin Drug Metab Toxicol*, 3(2):235–49, 2007.
- [18] Masoud Jamei. Recent advances in development and application of physiologically-based pharmacokinetic (pbpk) models: a transition from academic curiosity to regulatory acceptance. *Current pharmacology reports*, 2:161–169, 2016.

- [19] Manuela Grimstein, Yuching Yang, Xinyuan Zhang, Joseph Grillo, Shiew-Mei Huang, Issam Zineh, and Yaning Wang. Physiologically Based Pharmacokinetic Modeling in Regulatory Science: An Update From the U.S. Food and Drug Administration’s Office of Clinical Pharmacology. *Journal of Pharmaceutical Sciences*, 108(1):21–25, January 2019.
- [20] Nikolaos Tsamandouras, Thierry Wendling, Amin Rostami-Hodjegan, Aleksandra Galetin, and Leon Aarons. Incorporation of stochastic variability in mechanistic population pharmacokinetic models: handling the physiological constraints using normal transformations. *Journal of Pharmacokinetics and Pharmacodynamics*, 42(4):349–373, August 2015.
- [21] Amin Rostami-Hodjegan. Reverse Translation in PBPK and QSP: Going Backwards in Order to Go Forward With Confidence. *Clinical Pharmacology & Therapeutics*, 103(2):224–232, 2018.
- [22] Jane P. F. Bai, Ioannis N. Melas, Junguk Hur, and Ellen Guo. Advances in omics for informed pharmaceutical research and development in the era of systems medicine. *Expert Opinion on Drug Discovery*, 13(1):1–4, 2018. PMID: 29073782.
- [23] Kosuke Doki, Adam S. Darwich, Brahim Achour, Aleksi Tornio, Janne T. Backman, and Amin Rostami-Hodjegan. Implications of intercorrelation between hepatic cyp3a4-cyp2c8 enzymes for the evaluation of drug-drug interactions: a case study with repaglinide. *British journal of clinical pharmacology*, 84(5):972–986, 2018.
- [24] Maria Garcia-Cremades, Nicola Melillo, Iñaki F. Troconiz, and Paolo Magni. Mechanistic Multiscale Pharmacokinetic Model for the Anticancer Drug 2’,2’-difluorodeoxycytidine (Gemcitabine) in Pancreatic Cancer. *Clinical and Translational Science*, XX, 2020.
- [25] A. Rowland, M. van Dyk, A. M. Hopkins, R. Mounzer, T. M. Polasek, A. Rostami-Hodjegan, and M. J. Sorich. Physiologically based pharmacokinetic modeling to identify physiological and molecular characteristics driving variability in drug exposure. *Clin Pharmacol Ther*, 104(6):1219–1228, 2018.
- [26] Ilya M. Sobol. Sensitivity Estimates for Nonlinear Mathematical Models. *Mathematical modelling and computational experiments*, 1(4):407–414, 1993.
- [27] Andrea Saltelli. Making best use of model evaluations to compute sensitivity indices. *Computer Physics Communications*, 145(2):280–297, May 2002.
- [28] Andrea Saltelli, Marco Ratto, Terry Andres, Francesca Campolongo, Jessica Cariboni, Debora Gatelli, Michaela Saisana, and Stefano Tarantola. *Global Sensitivity Analysis. The Primer*. John Wiley & Sons, Ltd, January 2008.
- [29] Jeremy E. Oakley and Anthony O’Hagan. Probabilistic sensitivity analysis of complex models: a Bayesian approach. *Journal of the Royal Statistical Society: Series B (Statistical Methodology)*, 66(3):751–769, 2004. _eprint: <https://rss.onlinelibrary.wiley.com/doi/pdf/10.1111/j.1467-9868.2004.05304.x>.
- [30] Bertrand Iooss and Clementine Prieur. Shapley effects for sensitivity analysis with correlated inputs: comparisons with Sobol indices, numerical estimation and applications. *International Journal for Uncertainty Quantification*, 9(5), 2019. Publisher: Begel House Inc.
- [31] Dan Liu, Linzhong Li, Amin Rostami-Hodjegan, Frederic Y. Bois, and Masoud Jamei. Considerations and Caveats when Applying Global Sensitivity Analysis Methods to Physiologically Based Pharmacokinetic Models. *The AAPS Journal*, 22(5):93, July 2020.
- [32] Thierry A. Mara, Stefano Tarantola, and Paola Annoni. Non-parametric methods for global sensitivity analysis of model output with dependent inputs. *Environmental Modelling & Software*, 72:173 – 183, 2015.
- [33] Nhu Cuong Do and Saman Razavi. Correlation Effects? A Major but Often Neglected Component in Sensitivity and Uncertainty Analysis. *Water Resources Research*, 56(3):e2019WR025436, 2020. _eprint: <https://agupubs.onlinelibrary.wiley.com/doi/pdf/10.1029/2019WR025436>.
- [34] Sebastien Da Veiga, Francois Wahl, and Fabrice Gamboa. Local Polynomial Estimation for Sensitivity Analysis on Models With Correlated Inputs. *Technometrics*, 51(4):452–463, November 2009.
- [35] Genyuan Li, Herschel Rabitz, Paul E. Yelvington, Oluwayemisi O. Oluwole, Fred Bacon, Charles E. Kolb, and Jacqueline Schoendorf. Global Sensitivity Analysis for Systems with Independent and/or Correlated Inputs. *The Journal of Physical Chemistry A*, 114(19):6022–6032, May 2010.
- [36] C. Xu and G. Gertner. Extending a global sensitivity analysis technique to models with correlated parameters. *Computational Statistics & Data Analysis*, 51(12):5579–5590, August 2007.
- [37] S. Kucherenko, S. Tarantola, and P. Annoni. Estimation of global sensitivity indices for models with dependent variables. *Computer Physics Communications*, 183(4):937–946, April 2012.

- [38] S. Tarantola and Thierry A. Mara. Variance-based sensitivity indices of computer models with dependent inputs: the Fourier amplitude sensitivity test. *International Journal for Uncertainty Quantification*, 7(6), 2017. Publisher: Begel House Inc.
- [39] CERTARA L.P. Simcyp Simulator - Version 19, 2019.
- [40] Emanuele Borgonovo and Elmar Plischke. Sensitivity analysis: A review of recent advances. *European Journal of Operational Research*, 248(3):869–887, February 2016.
- [41] Francesca Pianosi, Keith Beven, Jim Freer, Jim W. Hall, Jonathan Rougier, David B. Stephenson, and Thorsten Wagener. Sensitivity analysis of environmental models: A systematic review with practical workflow. *Environmental Modelling & Software*, 79:214–232, May 2016.
- [42] Bertrand Iooss and Paul Lemaître. A Review on Global Sensitivity Analysis Methods. In *Uncertainty Management in Simulation-Optimization of Complex Systems*, Operations Research/Computer Science Interfaces Series, pages 101–122. Springer, Boston, MA, 2015.
- [43] E. S. Kostewicz, L. Aarons, M. Bergstrand, M. B. Bolger, A. Galetin, O. Hatley, M. Jamei, R. Lloyd, X. Pepin, A. Rostami-Hodjegan, E. Sjogren, C. Tannergren, D. B. Turner, C. Wagner, W. Weitschies, and J. Dressman. Pbpk models for the prediction of in vivo performance of oral dosage forms. *Eur J Pharm Sci*, 57:300–21, 2014.
- [44] John C. Loehlin and A. Alexander Beaujean. *Latent Variable Models: An Introduction to Factor, Path, and Structural Equation Analysis*. Routledge, New York, fifth edition edition, 2017.
- [45] Timothy A. Brown. *Confirmatory Factor Analysis for Applied Research*. Guilford Press, New York, second edition edition, January 2015.
- [46] Aleksandra Galetin, Caroline Brown, David Hallifax, Kiyomi Ito, and J. Brian Houston. Utility of recombinant enzyme kinetics in prediction of human clearance: Impact of variability, cyp3a5, and cyp2c19 on cyp3a4 probe substrates. *Drug Metabolism and Disposition*, 32(12):1411–1420, 2004.
- [47] J. N. Roy, J. Lajoie, L. S. Zijenah, A. Barama, C. Poirier, B. J. Ward, and M. Roger. Cyp3a5 genetic polymorphisms in different ethnic populations. *Drug Metab Dispos*, 33(7):884–7, 2005.
- [48] O. Lolodi, Y. M. Wang, W. C. Wright, and T. Chen. Differential regulation of cyp3a4 and cyp3a5 and its implication in drug discovery. *Curr Drug Metab*, 18(12):1095–1105, 2017.
- [49] Toshimitsu Homma and Andrea Saltelli. Importance measures in global sensitivity analysis of nonlinear models. *Reliability Engineering & System Safety*, 52(1):1–17, April 1996.
- [50] Andrew M. Farrell. Insufficient discriminant validity: A comment on bove, pervan, beatty, and shiu (2009). *Journal of Business Research*, 63(3):324 – 327, 2010.
- [51] Claes Fornell and David F. Larcker. Evaluating Structural Equation Models with Unobservable Variables and Measurement Error. *Journal of Marketing Research*, 18(1):39–50, 1981. Publisher: American Marketing Association.
- [52] Leonid M. Berezhkovskiy. A Valid Equation for the Well-Stirred Perfusion Limited Physiologically Based Pharmacokinetic Model that Consistently Accounts for the Blood–Tissue Drug Distribution in the Organ and the Corresponding Valid Equation for the Steady State Volume of Distribution. *Journal of Pharmaceutical Sciences*, 99(1):475–485, January 2010.
- [53] Michaela Vossen, Michael Sevestre, Christoph Niederal, In-Jin Jang, Stefan Willmann, and Andrea N. Edginton. Dynamically simulating the interaction of midazolam and the CYP3A4 inhibitor itraconazole using individual coupled whole-body physiologically-based pharmacokinetic (WB-PBPK) models. *Theoretical Biology and Medical Modelling*, 4(1):13, March 2007.
- [54] Michaelis L. and Menten M.L. Die Kinetik der Invertinwirkung. *Biochemistry Zeitung*, 49:333 – 369, 1913.
- [55] Amin Rostami-Hodjegan and Geoffrey T. Tucker. Simulation and prediction of in vivo drug metabolism in human populations from in vitro data. *Nature Reviews Drug Discovery*, 6(2):140–148, February 2007. Number: 2 Publisher: Nature Publishing Group.
- [56] Malcolm Rowland and Thomas N. Tozer. *Clinical Pharmacokinetics: Concepts and Applications*. Lippincott Williams & Wilkins, third edition, 1995.
- [57] E. Cacciari, S. Milani, A. Balsamo, E. Spada, G. Bona, L. Cavallo, F. Cerutti, L. Gargantini, N. Greggio, G. Tonini, and A. Cicognani. Italian cross-sectional growth charts for height, weight and BMI (2 to 20 yr). *Journal of Endocrinological Investigation*, 29(7):581–593, July 2006.
- [58] World Health Organization (WHO). *Body Mass Index - BMI*, (accessed September 28, 2020), 2020. <https://www.euro.who.int/en/health-topics/disease-prevention/nutrition/a-healthy-lifestyle/body-mass-index-bmi>.

- [59] Helen E. Cubitt, Karen R. Yeo, Eleanor M. Howgate, Amin Rostami-Hodjegan, and Zoe E. Barter. Sources of interindividual variability in IVIVE of clearance: an investigation into the prediction of benzodiazepine clearance using a mechanistic population-based pharmacokinetic model. *Xenobiotica*, 41(8):623–638, August 2011. Publisher: Taylor & Francis _eprint: <https://doi.org/10.3109/00498254.2011.560294>.
- [60] CERTARA L.P. Simcyp Simulator - Version 17, April 2017.
- [61] Brahim Achour, Matthew R. Russell, Jill Barber, and Amin Rostami-Hodjegan. Simultaneous Quantification of the Abundance of Several Cytochrome P450 and Uridine 5'-Diphospho-Glucuronosyltransferase Enzymes in Human Liver Microsomes Using Multiplexed Targeted Proteomics. *Drug Metabolism and Disposition*, 42(4):500–510, April 2014.
- [62] The MathWorks. MATLAB R2019b, the Mathworks, inc., Natick, Massachusetts, United States, 2019.
- [63] S. Marelli and B. Sudret. UQLab: a framework for uncertainty quantification in MATLAB. In *Proc. 2nd Int. Conf. on Vulnerability, Risk Analysis and Management (ICVRAM2014)*, Liverpool, United Kingdom, 2014.
- [64] M. E. (Bette) Meek, Hugh A. Barton, Jos G. Bessems, John C. Lipscomb, and Kannan Krishnan. Case study illustrating the WHO IPCS guidance on characterization and application of physiologically based pharmacokinetic models in risk assessment. *Regulatory Toxicology and Pharmacology*, 66(1):116–129, June 2013.
- [65] International Programme on Chemical Safety (IPCS). Characterization and Application of Physiologically Based Pharmacokinetic Models in Risk Assessment. Harmonization Project Document 9, World Health Organization (WHO), 2010.
- [66] Helen Graham, Mike Walker, Owen Jones, James Yates, Aleksandra Galetin, and Leon Aarons. Comparison of in-vivo and in-silico methods used for prediction of tissue: plasma partition coefficients in rat. *Journal of Pharmacy and Pharmacology*, 64(3):383–396, 2012.
- [67] Leonid M. Berezhkovskiy. Volume of Distribution at Steady State for a Linear Pharmacokinetic System with Peripheral Elimination. *Journal of Pharmaceutical Sciences*, 93(6):1628–1640, June 2004.
- [68] Patrick Poulin and Frank-Peter Theil. Prediction of pharmacokinetics prior to in vivo studies. 1. Mechanism-based prediction of volume of distribution. *Journal of Pharmaceutical Sciences*, 91(1):129–156, January 2002.
- [69] Stefan Willmann, Karsten Höhn, Andrea Edginton, Michael Sevestre, Juri Solodenko, Wolfgang Weiss, Jörg Lippert, and Walter Schmitt. Development of a Physiology-Based Whole-Body Population Model for Assessing the Influence of Individual Variability on the Pharmacokinetics of Drugs. *Journal of Pharmacokinetics and Pharmacodynamics*, 34(3):401–431, June 2007.
- [70] Ronald P. Brown, Michael D. Delp, Stan L. Lindstedt, Lorenz R. Rhomberg, and Robert P. Beliles. Physiological Parameter Values for Physiologically Based Pharmacokinetic Models. *Toxicology and Industrial Health*, 13(4):407–484, July 1997.
- [71] Trudy Rodgers, David Leahy, and Malcolm Rowland. Physiologically Based Pharmacokinetic Modeling 1: Predicting the Tissue Distribution of Moderate-to-Strong Bases. *Journal of Pharmaceutical Sciences*, 94(6):1259–1276, June 2005.
- [72] Trudy Rodgers and Malcolm Rowland. Physiologically based pharmacokinetic modelling 2: Predicting the tissue distribution of acids, very weak bases, neutrals and zwitterions. *Journal of Pharmaceutical Sciences*, 95(6):1238–1257, June 2006.
- [73] Axel Heinemann, Friedel Wischhusen, Klaus Püschel, and Xavier Rogiers. Standard liver volume in the caucasian population. *Liver Transplantation and Surgery*, 5(5):366–368, 1999.
- [74] J. Valetin. Basic Anatomical and Physiological Data for Use in Radiological Protection: Reference Values. Technical Report 89, International Commission on Radiological Protection (ICRP), 2002.
- [75] MJE Brill, PAJ Väitalo, AS Darwich, B van Ramshorst, HPA van Dongen, A Rostami-Hodjegan, M Danhof, and CAJ Knibbe. Semiphysiologically based pharmacokinetic model for midazolam and cyp3a mediated metabolite 1-oh-midazolam in morbidly obese and weight loss surgery patients. *CPT: Pharmacometrics & Systems Pharmacology*, 5(1):20–30, 2016.
- [76] Open Systems Pharmacology (OSP). OSP Suite - Version 7.1, (<http://www.open-systems-pharmacology.org/>), 2017.